

# On the use of acoustic records for the automatic detection and early warning of rockfalls

**G Olivieri** *GeCo S.r.l., Italy*

**S Vezzosi** *GeCo S.r.l., Italy*

**P Farina** *Geoapp S.r.l., Italy*

**L Meier** *Geopraevent AG, Switzerland*

## Abstract

*Infrasonic array technology has been widely used in the last years for the automatic detection and warning of snow avalanches and operative applications exist in Switzerland, Norway and British Columbia. The authors are currently investigating the capabilities of such a technology for the detection of rockfalls and its use as an early warning system to manage the risk associated with the occurrence of those events along linear infrastructures, such as roads and railways, and in open pit mines. The scientific literature clearly shows infrasonic array technology has excellent potential for the detection of rock mass flows such as debris flow events, but it is scarce in the field of rockfalls where the seismic methodology dominates. A first experimental campaign has been carried out by the authors on a site in the Swiss Alps to collect the acoustic (seismic and infrasonic) signature of a significant number of rockfall events and precisely characterise the associated wavefield in terms of frequency content and amplitude. The acoustic recordings have been compared with independent information collected by a Doppler radar installed on the same site and used operationally to close the access to the road located at the bottom of the slope. This paper presents the preliminary results of the above-described experimental campaign.*

**Keywords:** *rockfalls, acoustic measurement, seismic, early warning system*

## 1 Introduction

Rockfalls consist of the detachment of a rock or a few single rocks from a slope that is so steep that the rock continues to move down the slope, with movement characterised by free falling, bouncing, rolling and sliding phases (Ritchie 1963). Rockfall hazard cause serious safety concerns for linear infrastructures, such as transportation routes (railway lines, roads, pipelines etc.), located in areas prone to rockfalls (Lan et al. 2007; Yan et al. 2019) and also in open pit mines threatening human lives, machinery and portal structures located at the toe of highwalls (Alejano et al. 2007, 2008; Giacomini et al. 2011). In addition to the safety concerns, rockfall events also cause serious disruption to the operations of both linear infrastructures and open pit mines, resulting in significant financial losses. The occurrence of 238 rockfalls at 214 sites along the 1,134 km long Chengdu-Kunming Railway (Yan et al. 2019) gives an idea of the degree of risk of line closure (910 hours of 16 minute traffic interruptions) and consequent economic losses associated with the occurrence of rockfalls. Once a rockfall hazard assessment—aimed at identifying the temporal probability and the spatial susceptibility of rockfall events, the trajectory and maximum runout of falling blocks and the distribution of rockfall intensity—has been carried out, different strategies are commonly used to reduce or mitigate the identified hazard. The most common strategies are represented by a benched slope design, especially in open pit mines, combined with catch benches/berms, and rockfall structural protection systems, such as draped meshes, spot bolts, cable lashing, fences, dynamic barriers, up to galleries and embankments. These countermeasures are expensive and often not able to provide complete protection from rockfalls. Automatic early warning systems that are able to operate autonomously in challenging environments and over large areas, allowing efficient, low-cost gathering and transfer of the acquired data are therefore strongly requested in these areas.

The sudden nature of rockfall events which typically lack significant precursor deformations and their small and widespread spatial distribution over the slopes where potential source areas are located, make it extremely difficult to detect their occurrence and to generate timely warnings to reduce the exposure to risk of personnel, machinery, cars and trains located in the potential run out area. Along railways many areas with frequent rockfall events are protected by wire fences, which provide warnings for such events but the proximity of the fences to the train line does not allow sufficient warning and reaction time for approaching trains. Video image recognition is susceptible to environmental constraints such as poor performance at night, in heavy fog and during extreme rainfall conditions. To date, Doppler radar and seismic technology seem to be the two most promising technologies to provide early warnings for rockfall events thanks to their short response time and their capabilities to work remotely and in any weather conditions.

Radar technology enables location and tracking of rockfalls in real time at long distances from the radar location (e.g. 1–2 km) that fall within the radar field of view (e.g. 90° vertical and 20° horizontal). It provides timely alerts (a few seconds after detachment) even in the event of small boulders. Radar can provide the location of the source areas, the rock velocity, the travel path, the runout distance, an estimation of the size of the rockfall and the deposit area (Meier et al. 2017). Given the reliability of the measurements, this technology currently represents an operational solution to cover specific sectors of the slope prone to rockfalls facilitating automatic closure of roads (Geopraevent AG c. 2020).

The seismic signals generated by rockfalls and larger mass movements have been extensively investigated in different geotechnical contexts showing that rockfalls generate seismic waves and that the recorded signal can provide important information associated with the volume, duration and extent of rockfall events (Norris 1994; Deparis et al. 2008; Vilajosana et al. 2008; Dammeier et al. 2011; Hibert et al. 2011, 2017; Surinach et al. 2005). The use of a networks of seismic sensors close (~1 km) to the source area (Lacroix & Helmstetter 2011; Zimmer & Sitar 2015; Dietze et al. 2017) offers the opportunity to precisely locate and track rockfalls which in turn strongly improve the capability of the method to filter out seismic events of different nature (earthquakes, trains, noise etc.) and the reliable automatic detection and early warning of rockfall events. The use of an array composed of no. 6 geophones with 10 m spacing deployed by the side of railways (Collins et al. 2014) allowed the automatic detection of the impact of rockfalls of even a small size (100–200 kg) over a short portion of the railway. Three small-aperture (100–300 m) seismic arrays of seven seismometers were deployed 100–500 m from the Séchilienne rockslide on the French Alps (Lacroix & Helmstetter 2011) and are able to accurately locate the rockfall impacts as well as measure the trajectory and propagation speed and the microearthquakes activity within the most active part of the rockslide. A network of six seismic sensors deployed around a 2 km<sup>2</sup> large near-vertical cliff section in the Swiss Alps revealed a powerful method to locate small (0.2 m<sup>3</sup>) to medium sized (2 m<sup>3</sup>) rockfalls events (Dietze et al. 2017) occurred within the network. The measurements of Zimmer & Sitar (2015) indicated infrasound signal produced by rockfalls is viable and complementary to seismic specially to provide insights on the source location and on the points of impact if multiple measurements stations are used. Infrasonic technology has proven to be a reliable tool for the monitoring of mass flows such as debris flow (Marchetti et al. 2019) and avalanches (Ulivieri et al. 2011; Marchetti et al. 2015) and some operative applications for the automatic detections and early warning of avalanches occurrence over large (2–5 km) areas already exists (Steinkogler et al. 2018; Mayer et al. 2018), but the literature related to infrasound and rockfalls is still scarce.

In this paper we are analysing the seismic and infrasonic signals generated by 91 rockfall events of different volumes occurred in the period 20 July 2019 to 13 August 2019 over a test site represented by a natural slope located above the village of Brinzauls, in the Swiss Alps, where rockfalls frequently occur. These seismic and infrasonic signals were compared with the information collected by a Doppler radar and webcam installed on the same test site for operational purposes. The goal of this investigative campaign was to characterise the seismic and infrasonic wavefields of different sized rockfall events and evaluate the feasibility of an effective acoustic rockfalls detection in terms of distance range and size.

## 2 Acoustic experimental set-up

Since mid-December 2018, a Doppler radar operates in Brinzauls, Switzerland, to permanently monitor a rockfall zone at a distance of  $\sim 1$  km and automatically closes the main road at the bottom of the slope when rockfall events (Figure 1). The radar is coupled with a webcam, able to automatically record the events detected by the radar (Figure 1). The radar operates 24/7 in any weather conditions and provides precise measurement of the occurrence time, area, duration and runout distance of all the movements occurring within the field of view (Figure 1, dotted red circular sector).

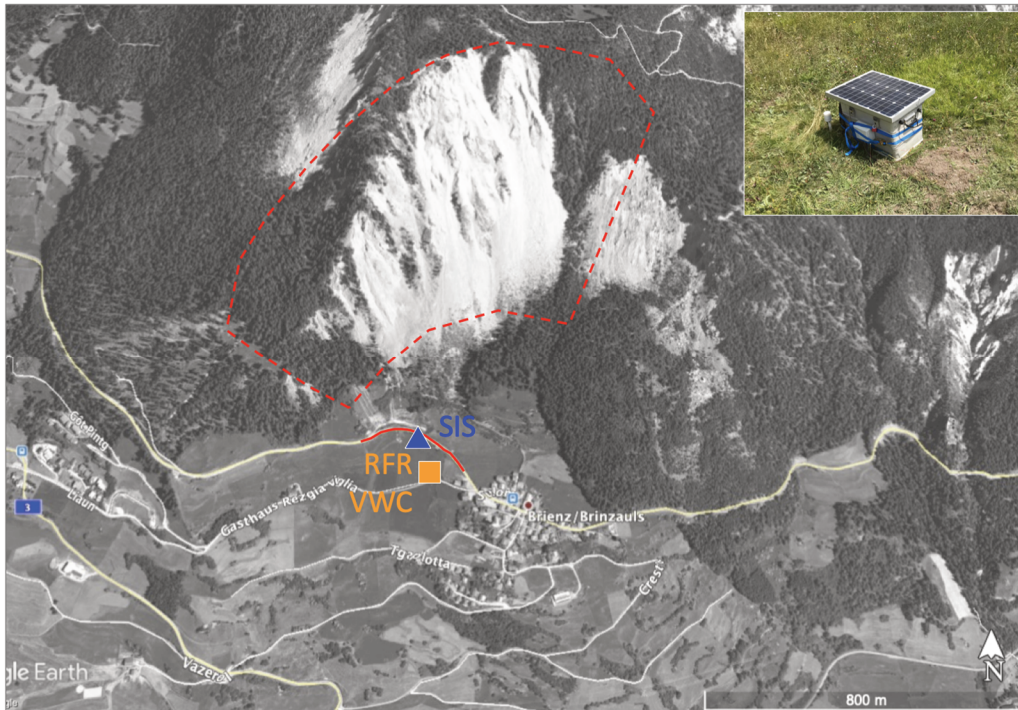


**Figure 1** Map of the experimental site with position of the seismo-infrasonic station (SIS), rockfall radar (RFR) and visible webcam (VWC). The rockfall source sector monitored by the radar (dotted red polygon) and the portion of road exposed to falling rocks (red line) are also shown. A photo of the seismo-infrasonic station is shown on the inset

In July 2019, a seismo-infrasonic station (SIS) was installed close to the radar (Figure 1). The station is equipped with a 24 bit/250 Hz digital acquisition station (CMG-DM24-S3), a 3D seismic sensor (CMG-6T) and a highly sensitive (400 mV/Pa) differential pressure sensor. Data were continuously transmitted in real time via a 3G modem. For this initial data acquisition campaign, the station was installed very close ( $\sim 10$  m) to the road for logistical and safety reasons where a strong exposure of the sensors to vehicle traffic noise was expected. Seismic, infrasonic and visible camera information were synchronised using a GPS sensor.

## 3 Acoustic record of a large rockfall event

Since the initial installation of the acoustic station, the Doppler radar detected a significant number of rockfalls. On 13 August 2019 at 14:03:37 local time the radar automatically closed the road after having detected a large ( $44 \text{ m}^3$ ) boulder that fell down from the upper part of the slope, had a run out of more than 1 km, and hit the road (Figure 2) stopping approximately 40 m from the acoustic station. The radar estimated an average velocity of the block of 59 km/h. The total duration of the event was 82 seconds (Figure 2). The webcam images clearly showed the boulder (Figure 2, white arrow) providing the exact timing of when the boulder reached the road (Figure 2, white arrows). This occurred 48 seconds after the automatic road closure triggered by the radar.

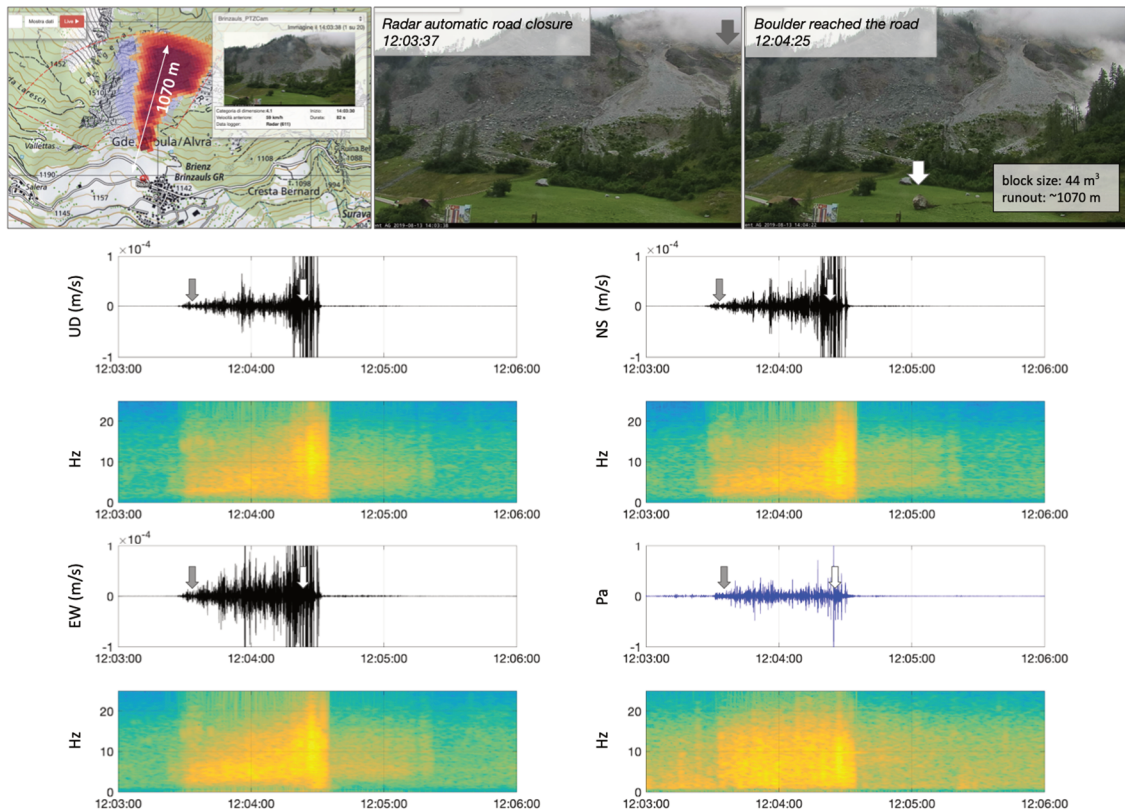


**Figure 2** Radar outputs (top left), visible video images (top middle and right), seismic (up–down (UD), north–south (NS) and east–west (EW), black traces) and infrasonic (blue trace) records with respective spectrograms (coloured images) of the large rockfalls event on 13 August 2019 at 14:03:37 local time. Grey and white arrows indicate the radar automatic road closure and boulder close (20–30 m) the road times, respectively

A clear seismic as well as infrasonic signal is generated by this large rockfall event (Figure 2). Both signals show a similar duration of one minute and start with low amplitude which increases with time and reach peak amplitude when the boulder is passing in proximity to the sensor (Figure 2, black traces). The average seismic root mean square (RMS) amplitude is  $14 \mu\text{m/s}$  (UD component) while peak values of  $\sim 1,500 \mu\text{m/s}$  (UD component). The average infrasonic RMS amplitude is  $53 \text{ mPa}$  with peak values of  $1.5 \text{ Pa}$  (Figure 2c, blue trace). Once the boulder stopped the seismic and infrasonic signals lasted a further  $\sim 50$  seconds with an RMS amplitude strongly reduced to  $0.4 \mu\text{m/s}$  and  $3.5 \text{ mPa}$ , respectively, which reflect the dynamics of the debris flow associated with the event. The spectral analysis of the seismic and infrasonic signals shows frequency content between 2 and 15 Hz (Figure 2, coloured images) with similar increasing trend with time. Spectral analysis also indicates a higher signal-to-noise ratio of the seismic recordings with respect to the infrasonic one.

The initial part of both seismic and infrasonic signals is emergent and the onset precedes the radar alert time of approximately 9 and 7.5 seconds (Figure 3), respectively, indicating both signals are emitted from the early stages of the detachment. Discrete impulses emerging from the background signal are evident on the infrasonic record since the beginning (Figure 3) and during most of the signal (Figure 2, blue trace), while the presence of discrete impulses on the seismic signal is observable only when the phenomenon approaches ( $< 200 \text{ m}$ ) the station (Figure 2, black traces). The observed  $\sim 2.5$  seconds long delay between the seismic and infrasonic onset (Figure 3, dotted lines) reflects the different propagation velocity of the acoustic waves in the ground and in the atmosphere. Assuming the seismic and infrasonic sources located at the same distance ( $\sim 800 \text{ m}$ ) and the sound velocity of  $340 \text{ m/s}$ , the resulting seismic group velocity ranges from  $650$  to  $700 \text{ m/s}$ , which is compatible with seismic velocities at shallow depth and in presence of soft deposits.



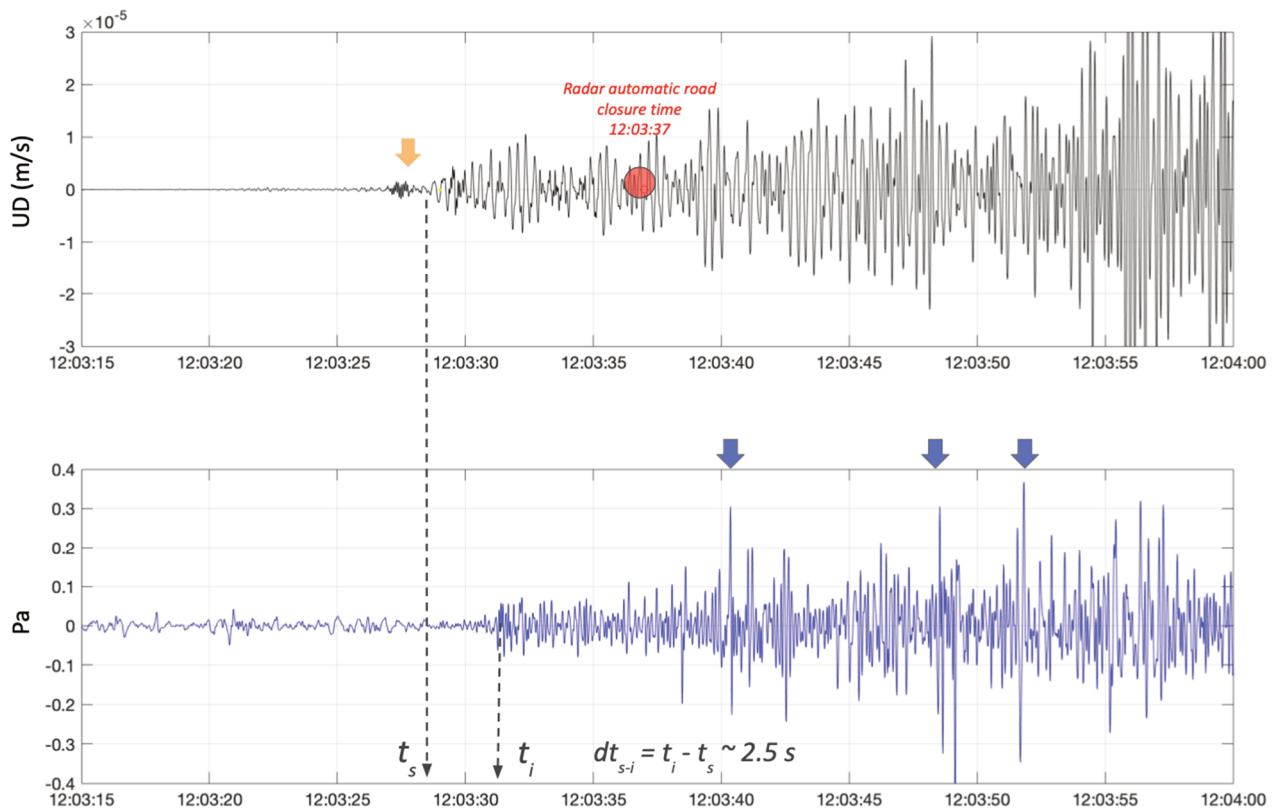


Figure 3 A 30-second zoom of the initial part of the seismic (black) and infrasonic (blue) records associated with the large rockfalls event on 13 August 2019 at 14:03:37 local time (UTC + 02:00). Dotted lines indicate the seismic and infrasonic onset and the red circle indicates the automatic road closure time. Blue arrows indicate infrasonic impulsive phases

#### 4 Assessment of the capabilities of acoustic signal to detect rockfalls

During the first ~3 weeks of operation of the acoustic station (18 July 2019 to 13 August 2019), the Doppler radar automatically detected 91 rockfall events of various size, whose occurrence times were used to extract a statistically significant number acoustic signals.

The radar provides an estimation of the event size based on an empirical combination of the dimension of the moving areas as well as the signal power and velocity. Starting from the area where movement was detected by the radar, for each event we estimated the runout distance, which more closely reflects the potential energy associated with the event. For each rockfall event detected by the radar we then computed the seismic and infrasonic RMS amplitude.

The analysed rockfalls events cover a wide range of runout distances (70–1,070 m), associated with the detachment of small blocks that stop immediately (~100 m) to the rolling of large blocks that cover about 1 km, reaching the road located at the bottom of the slope. The seismic (UD) and infrasonic RMS amplitudes ranges respectively from 0.01 to 14  $\mu\text{m/s}$  (Figure 4, black squares) and 5 to 52 mPa (Figure 4, blue circles), increasing with the increase of the runout distance (Figure 4, upper plot). A general increase in seismic and infrasonic amplitude with increasing distance travelled by blocks is observable.

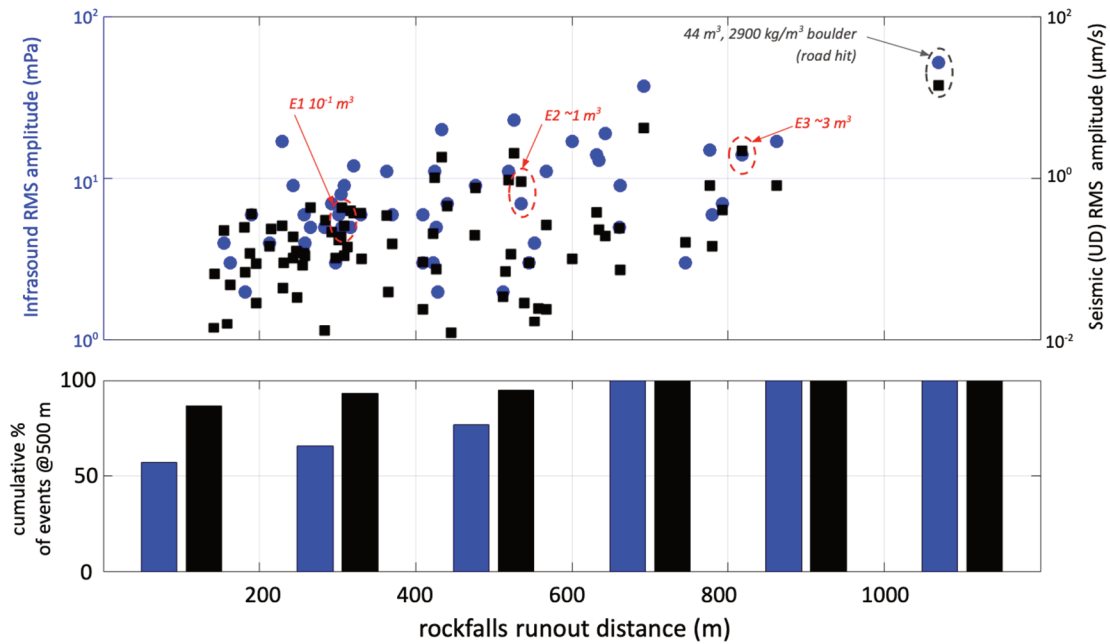


**Figure 4** Upper plot: Seismic (#79) and infrasonic (#52) RMS amplitudes rockfalls events detected by Doppler radar as a function of the estimated rockfalls runout distance. Lower plot: cumulative percentage of the number of seismic (black) and infrasonic (blue) recorded signals with respect to those detected by the Doppler radar as a function of the runout distance

The percentage of events clearly detected by the acoustic sensor, with respect to those detected by the radar as a function of the runout distance, indicates that for events with runout distance larger than ~600 m both seismic and infrasonic detection capability is 100%. For smaller runout events the acoustic efficiency decreases and, as expected, the elastic energy is transmitted more efficiently into the ground than into the atmosphere (Figure 4).

The analysis of the webcam images with good visibility, allowed the estimation of the order of magnitude of the rock blocks volume associated with some events (Figure 5). A general increasing trend of the amplitude of the seismic and infrasonic signals is observable with increasing volume of the falling blocks (Figures 4 and 5 dotted red circles). The fall of an estimated 1 m<sup>3</sup> block travelling a distance of approximately 500 m produces an effective and well detectable acoustic wavefield, in particular seismic, while the energy produced is generally weak and less detectable for small sized block (~0.1 m<sup>3</sup>, <300 m run-out distance).

Within the general increasing trend of seismic and infrasonic efficiency with increasing volume and distance travelled by rock blocks, a wide variability of amplitudes related to events with same runout distance and/or blocks volumes is observed. This indicates that the effectiveness of the acoustic source is not only linked to the size of the blocks and that further factors (number of slots, rolling, bouncing etc.) may influence the acoustic efficiency.

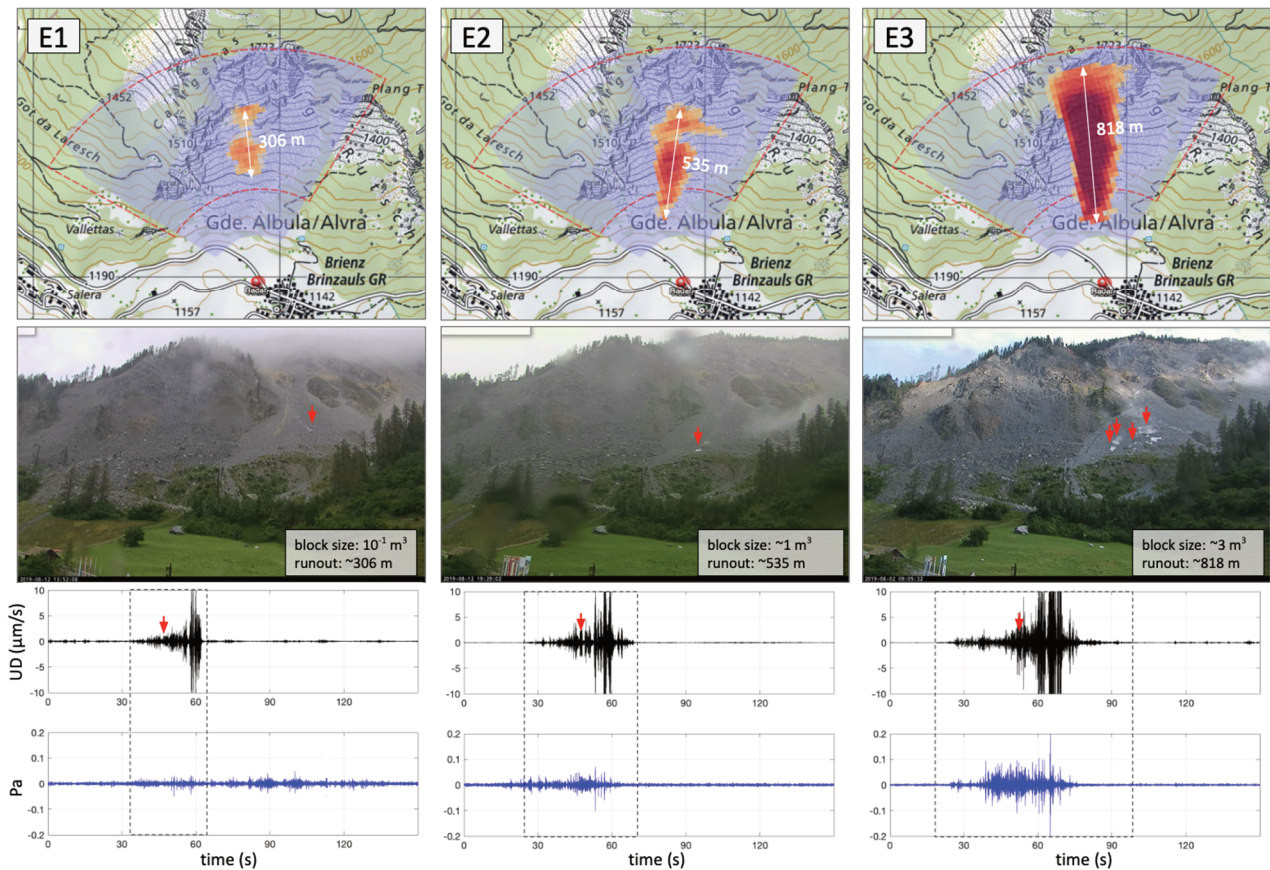


Figure 5 Visible images (top) and relative seismic (black) and infrasonic (blue) signals (bottom) of three rockfalls events that occurred on the same sector and with increasing runout distance and size of the rolling blocks (red arrows and inlet info on the images). The red arrows on the records indicate the time the image was taken

## 5 Estimate of the expected acoustic detection range

The seismic and infrasonic RMS amplitudes of the three events with increasing blocks volume (Figure 6) recorded at an average distance of 500 m from the source area have been taken into account in order to estimate the expected amplitudes at distance using seismic and infrasound attenuation laws. The adopted seismic attenuation law contemplates both the geometrical spreading and intrinsic attenuation and scattering effects.

$$A_s(D) = A_{s500} \cdot D^{-1} \cdot e^{-\left(\frac{\pi f}{v \cdot Q_T} D\right)} \quad (1)$$

where  $A_{s500}$  is the seismic amplitude at 500 m of distance,  $D$  the distances,  $f$  the frequency,  $v$  the propagation velocity and  $Q_T$  the quality factor, while the infrasonic attenuation law contemplates only the distance.

$$A_i(D) = A_{i500} \cdot D^{-1}, \quad (2)$$

where  $A_{i500}$  is the recorded infrasound amplitude at 500 m distance. Assuming a seismic propagation velocity  $v$  of 700 m/s, a frequency content  $f$  of 6 Hz and a quality factor  $Q_T$  of 1000, the expected seismic and infrasonic amplitudes in the 0–8 km range is shown on Figure 6.

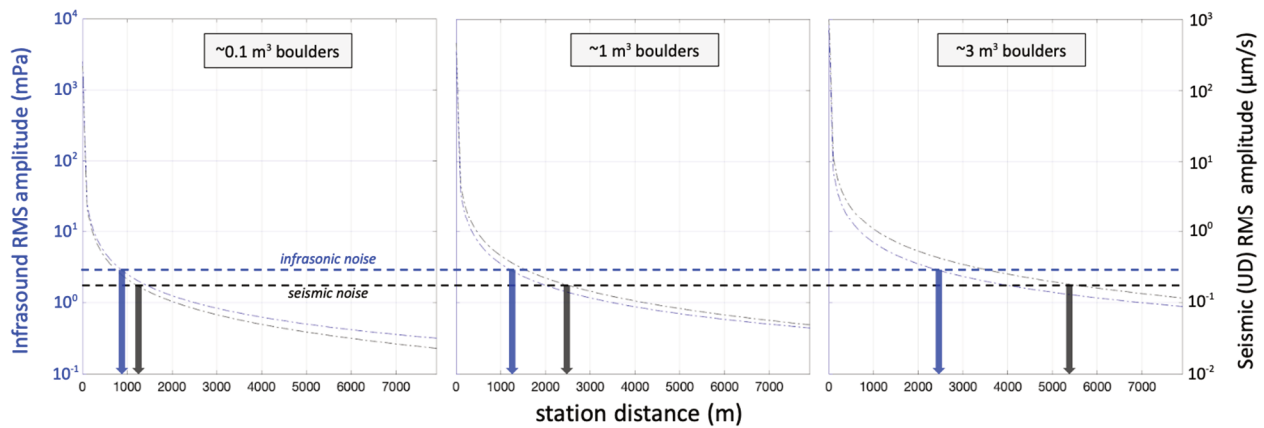


**Figure 6** Expected seismic (black) and infrasonic (blue) amplitude attenuation with distance for three order of magnitude ( $0.1$ ,  $1.0$  and  $3.0 \text{ m}^3$ ) block size. Black and blue dotted lines indicate the limits of seismic and infrasonic amplitude below which the signal to noise ratio does not allow an effective detection. Black and blue arrows indicate the expected seismic and infrasonic detection range, respectively

Considering both the sensor and site noise level and a signal-to-noise ratio of 2 (Figure 6, dotted horizontal lines), the expected seismic and infrasonic detectability range of small ( $\sim 0.1 \text{ m}^3$ ), medium ( $\sim 1 \text{ m}^3$ ), and large ( $\sim 3 \text{ m}^3$ ) block rock is  $0.8$ ,  $1.2$  and  $2.5 \text{ km}$  and  $1.2$ ,  $2.5$  and  $5.2 \text{ km}$ , respectively (Figure 6, black and blue arrows).

## 6 Conclusion

Seismic and highly sensitive infrasonic sensors were installed in a site in the Swiss Alps approximately  $700 \text{ m}$  away from an area where frequent rockfall phenomena occur in order to characterise the acoustic signature of rockfall events. Information on the size of these events (runout distance and block size) was provided by a Doppler radar and a camera installed on the same site. This provided indications both on the nature of the acoustic source of the rockfall phenomena and on the amount of acoustic energy associated with the size of these events.

The detachment of a large boulder ( $44 \text{ m}^3$ ,  $2,900 \text{ kg/m}^3$ ) that travelled  $\sim 1 \text{ km}$ , crossed the road located at the bottom of the slope and stopped at about  $40 \text{ m}$  from the station, generating a very clear seismic and infrasonic signal since the moment of detachment. Similar seismic and infrasonic signal duration ( $\sim 60$  seconds) and frequency content ( $2 \text{ Hz}$  to  $15 \text{ Hz}$ ) were observed, suggesting common source dynamics.

The analysis of the acoustic signals of 91 rockfall events of various sizes detected by the Doppler radar indicates that larger events associated with the detachment of rock blocks of the order of  $1.0$ – $3.0 \text{ m}^3$  and covering distances greater than  $500 \text{ m}$  produced a well detectable acoustic signals both in soil and in the atmosphere. As expected, the elastic energy is transmitted more efficiently into the ground than into the atmosphere. This order of magnitude of rockfall events generates a seismic and infrasonic signal which can also be recorded at distances of  $2$ – $3 \text{ km}$  from the source, revealing the potential of the acoustic method for the detection of rockfalls at long distances over a  $360$  degrees field of view. However, the use of a single station greatly reduces the reliability of the method for the automatic event detection because of the difficulties in separating the rockfall signal from the signal generated by other sources. Acoustic array or network techniques will be tested in the future to verify the effectiveness of this method as an automatic early warning system for rockfalls.

## Acknowledgement

The authors would like to thank the authorities of Brinzauls (Switzerland) and the Canton of Grisons to have given access to the site and support to install the acoustic station.



## References

- Alejano, L, Pons, B, Bastante, F, Alonso, E & Stockhausen, H 2007, 'Slope geometry design as a means for controlling rockfalls in quarries', *International Journal of Rock Mechanics and Mining Sciences*, vol. 44, no. 6, pp. 903–921.
- Alejano, L, Stockhausen, H, Alonso, E, Bastante, F & Ramírez-Oyanguren, P 2008, 'ROFRAQ: A statistics-based empirical method for assessing accident risk from rockfalls in quarries', *International Journal of Rock Mechanics and Mining Sciences*, vol. 45, no. 8, pp. 1252–1272.
- Collins, D, Toya, Y, Hosseini, Z & Trifu, C-I 2014, 'Real time detection of rockfall events using a microseismic railway monitoring system' *Geohazards*, vol. 6.
- Dammeier, F, Moore, JR, Haslinger, F & Loew, S 2011, 'Characterization of alpine rockslides using statistical analysis of seismic signals', *Journal of Geophysical Research*, vol. 116.
- Deparis, J, Jongmans, D, Cotton, F, Baillet, L, Thouvenot, F & Hantz, D 2008, 'Analysis of rock-fall and rock-fall avalanche seismograms in the French Alps', *Bulletin of the Seismological Society of America*, vol. 98, pp. 1781–1796.
- Dietze M, Mohadjer S, Turowski JM, Ehlers, TA & Hovius N 2017, 'Seismic monitoring of small alpine rockfalls validity, precision and limitations', *Earth Surface Dynamics*, vol. 5, pp. 653–668, <https://doi.org/10.5194/esurf-5-653-2017>
- Geoprevent AG ca. 2020, *Rockfall Radar Brienz*, Geopraevent AG, Zürich, viewed 3 March 2020, <https://www.geopraevent.ch/project/rockfall-radar-brienz/?lang=en>
- Hibert C, Malet, JP, Bourrier, F, Provost, F, Berger, F, Bornemann, P, Tardif, P & Mermin, E 2017, 'Single-block rockfall dynamics inferred from seismic signal analysis', *Earth Surface Dynamics*, vol. 5, pp. 283–292.
- Hibert C, Mangeney, A, Grandjean, G & Shapiro, NM 2011, 'Slope instabilities in Dolomieu crater, Réunion Island: From seismic signals to rockfall characteristics', *Journal of Geophysical Research*, vol. 116.
- Giacomini, A, Thoeni, K, Kniest, KE & Lambert, C 2011, 'In situ experiments of rockfall in open pit coal mine', in E Eberhardt & D Stead (eds), *Proceedings of the 2011 International Symposium on Slope Stability in Open Pit Mining and Civil Engineering*, Canadian Rock Mechanics Association.
- Lan, H, Martin, CD & Lim, CH 2007, 'Rockfall analyst: a GIS extension for three-dimensional and spatially distributed rockfall hazard modeling', *Computers & Geosciences*, vol. 33, pp. 262–279.
- Lacroix, P & Helmstetter, A 2011, 'Location of seismic signals associated with microearthquakes and rockfalls on the Sechilienne Landslide, French Alps', *Bulletin of the Seismological Society of America*, vol. 101, no. 1, pp. 341–353, <http://dx.doi.org/10.1785/0120100110>
- Marchetti, E, Walter, F, Barfucci, G, Genco, R, Wenner, M, Ripepe, M, McArdeell, B & Price, C 2019, 'Infrasound array analysis of debris flow activity and implication for early warning', *Journal of Geophysical Research: Earth Surface*, vol. 124.
- Marchetti, E, Ripepe, M, Ulivieri, G & Kogelnig, A 2015, 'Infrasound array criteria for automatic detection and front velocity estimation of snow avalanches: towards a real-time early-warning system', *Natural Hazards and Earth System Sciences*, vol. 15, no. 11, pp. 2545–2555.
- Mayer, S, Herwijnen, AV, Ulivieri, G & Schweizer, J 2018, 'Evaluating the performance of operational infrasound avalanche detection systems at three locations in the Swiss Alps during two winter seasons', *Proceedings of the International Snow Science Workshop*, pp. 611–615.
- Meier, L, Jacquemart, M, Wahlen, S & Blattmann, B 2017, 'Real-time rockfall detection with doppler radars', in J Corominas, J Moya & M Janeras (eds), *Proceedings of the 6th Interdisciplinary Workshop on Rockfall Protection*, International Center for Numerical Methods in Engineering, Barcelona, pp. 1–4.
- Norris, D 1994, 'Seismicity of rockfalls and avalanches at three cascade range volcanoes: implications for seismic detection of hazardous mass movements', *Bulletin of the Seismological Society of America*, vol. 84, no. 6, pp. 1925–1939.
- Ritchie, AM 1963, 'Evaluation of rockfall and its control', *Highway Research Record 17*, Highway Research Board, Washington, pp. 13–28.
- Steinkogler W, Ulivieri, G, Vezzosi, S, Hendrikx, J, Herwijnen & AV, Humstad, T 2018, 'Infrasound detection of avalanches: operational experience from 28 combined winter seasons and future developments', *Proceedings of the International Snow Science Workshop*, pp. 621–626.
- Surinach, E, Vilajosana, I, Khazaradze, B, Biescas, B, Furdada, G & Vilaplana, JM 2005, 'Seismic detection and characterization of landslides and other mass movements', *Natural Hazards and Earth System Sciences*, vol. 5, pp. 791–798.
- Ulivieri, G, Marchetti, E, Ripepe, M, Chiambretti, I, Rosa, GD & Segor, V 2011, 'Monitoring snow avalanches in northwestern Italian Alps using an infrasound array', *Cold Regions Science and Technology*, vol. 69, no. 2–3, pp. 177–183.
- Vilajosana, I, Surinach, E, Abellan, A, Khazaeadze, G, Garcia, D & Llosa, J 2008, 'Rockfall induced seismic signal: case study in Montserrat, Catalonia', *Natural Hazards and Earth System Sciences*, vol. 8, pp. 805–812.
- Yan, Y, Ting, L, Jie, L, Wubin, W & Qian, S 2019, 'Monitoring and early warning method for a rockfall along railways based on vibration signal characteristics', *Scientific Reports*, vol. 9, article number 6606.
- Zimmer, VL & Sitar, N 2015, 'Detection and location of rockfalls using seismic and infrasound sensors', *Engineering Geology*, vol. 193, pp. 49–60.

